The role of molecular defects on the structure and phase transitions of poly(vinylidene fluoride)

Andrew J. Lovinger, D. D. Davis, R. E. Cais and J. M. Kometani
AT&T Bell Laboratories, Murray Hill, NJ 07974, USA
(Received 7 August 1986; accepted 14 October 1986)

Having prepared poly(vinylidene fluoride) (PVF_2) with 0.2–23.5 mol% head–head/tail–tail (HHTT) defects (by comparison with the commonly obtainable 3.5–6.0 mol%), we examined the influence of such regiodefects on crystal structure, polymorphism and Curie transitions. The structure at ambient temperature changes from α to β as the HHTT content is increased beyond *ca.* 11.4 mol%. At that composition, either of these two phases may predominate, depending upon temperature of crystallization (higher ones favouring β). For defect contents over 15.5 mol%, the polymer chains show progressive *intra*molecular disorder, yet are packed with increasing *inter*molecular order in a pseudohexagonal lattice. When PVF_2 containing 13.5–15.5 mol% regiodefects is heated, clear ferroelectric–paraelectric phase transformations are obtained; these are reversible (with thermal hysteresis) upon subsequent cooling. This confirms our previous findings of Curie transitions in PVF_2 copolymers with tri-or tetra-fluoroethylene, and shows that such Curie behaviour is an inherent property of PVF_2 itself. No solid-state transformations were observed for polymers with over 15.5 mol% defects, their structure remaining akin to that of the paraelectric phase at all temperatures between -10°C and the melting point. Within the same temperature range, the essentially isoregic PVF_2 (0.2 mol% defects) remains predominately in the α-phase. On the other hand, the polymer having 11.4 mol% defects shows a remarkable transformation during heating, from the anti-polar α-phase to the paraelectric phase.

(Keywords: molecular defects; structure; phase transition; poly(vinylidene fluoride))

INTRODUCTION

Molecular defects are ubiquitous in poly(vinylidene fluoride) (PVF_2). They are introduced during free-radical polymerization when $CF_2{=}CH_2$ monomers are added onto the growing chain in an inverted manner rather than all in the same direction (isoregically)[1]. Such inverted addition normally takes place to an extent of *ca.* 3.5–6.0 mol% (depending upon temperature[2]), and leads to the well known head–head (HH) defects (i.e. $-CF_2-CF_2-$) and tail–tail (TT) defects (i.e. $-CH_2-CH_2-$)[3]. In PVF_2, head–head addition is normally followed by TT addition, so that the regiodefective units consist of HHTT sequences. Because the relative amount of such units cannot be varied substantially outside the 3.5–6.0 mol% range, their effects on crystal structure and phase transitions are not known. However, from the earliest days of research into PVF_2, this subject has aroused the interest of a number of investigators who have attempted to predict or simulate the effects of HHTT sequences. In an important paper dealing with conformational energetics of PVF_2, Farmer and co-workers[4] predicted that the antipolar α-phase (tg^+tg^- conformation) should be energetically favoured for HHTT contents below *ca.* 11 mol%, while the polar β-phase (all-*trans* conformation) should become the more stable polymorph when defects exceed *ca.* 11 mol%. Even though almost fifteen years have passed since publication of ref. 4, this prediction has still not been tested experimentally because PVF_2 with the required content of regiodefects had not been available until very recently[5]. However, in an early attempt to simulate the role of HH defects (in the absence of the accompanying TT units), Lando and Doll[6] copolymerized vinylidene fluoride with tetrafluoroethylene (F_4E) and showed a polymorphic change from α to β as the F_4E content exceeded *ca.* 7 mol%; this phase change was also substantiated by potential-energy calculations[4].

In addition to their role in determining polymorphism during crystallization, these HHTT defects could also be expected to play a role in Curie transitions or other phase transformations during heating or cooling. In fact, deliberate introduction of defects has been used extensively in the quest to discover such Curie transitions in PVF_2 and to elucidate their nature (see, for example, recent reviews[7–9]). The reason for this is that, although PVF_2 displays many characteristics of traditional ferroelectric materials (e.g. hysteresis of electric displacement with applied field)[10], no clear Curie transition is seen up to its melting region (*ca.* 175°C–185°C). While the earliest indications of an incipient ferroelectric–paraelectric transformation have been reported[11,12] just below the melting point (i.e. at *ca.* 172°C), no full transition is obtained since it is rapidly thwarted by melting. Moreover, the reverse transformation (paraelectric–ferroelectric) is not seen upon cooling because PVF_2 crystallizes with the antipolar α-phase.

On the other hand, Yagi and co-workers[13] showed that the introduction of trifluoroethylene (abbreviated F_3E) units to PVF_2 leads to a clear phase transformation during both heating and cooling, which has been

0032-3861/87/040617-10$03.00

unequivocally identified as a Curie transition[14-19]. The transition temperature increases with VF_2 content, and extrapolation to 100% PVF_2 indicates[19] that its Curie temperature is centred slightly above the melting point, which explains the fact that only an incipient transition is seen in PVF_2 before complete melting. While this transition in VF_2/F_3E copolymers is still eliciting great interest and yielding important new results (concerning, for example, the effects of poling[20], pressure[21,22] or irradiation[23,24]), we have recently focused on a different family of copolymers, i.e. those with tetrafluoroethylene (F_4E). As we have already discussed[25-27], F_4E does not cause the complications inherent in F_3E (i.e. introduction of a different chemical unit (–CHF–) and of concomitant stereoirregularity into its copolymers with PVF_2); instead, it simply increases the number of HH defects already present in PVF_2. Through study of such copolymers over the entire compositional range[25-27], we found clear (and reversible) Curie transitions for VF_2 contents between *ca.* 64 and 82 mol%; similar results have also recently been obtained by Murata and Koizumi[28]. These results confirmed our previous findings on the Curie transition, by showing that it is not uniquely associated with the F_3E comonomer, as well as by yielding an extrapolated Curie temperature for PVF_2 of 195°C–197°C, which is indeed slightly above the melting point.

However, while these VF_2/F_4E copolymers are much more akin to PVF_2 than were their VF_2/F_3E counterparts, they are still not its true regioisomers: the reason is that they introduce only the HH part of the defect, *but not the accompanying TT units* that typify the regiodefects in PVF_2. Consequently, the availability of PVF_2 with a variable amount of HHTT defects allows us for the first time to bypass all uncertainties associated with the comonomers (F_3E and F_4E) and to study directly the existence and nature of Curie (and other) transitions in PVF_2 as functions of regiodefect content.

EXPERIMENTAL

Isoregic PVF_2 was prepared by bulk polymerization of 1,1-dichloro-2,2-difluoroethylene, followed by reductive dechlorination with tri(n-butyl) tin hydride, as outlined previously[29]. Both the yield of the precursor polymer and the degree of polymerization are very low (i.e., *ca.* 3% and *ca.* 50, respectively). The ^{19}F n.m.r. spectra of this polymer obtained at 188 MHz show an HHTT defect content of 0.2% (expressed as in ref. 1).

Aregic PVF_2 having a variable defect content (from 11.4 to 23.5% HHTT) was synthesized by copolymerization of vinylidene fluoride with 1-chloro-2,2-difluoroethylene, followed once again by reductive dechlorination with tri(n-butyl) tin hydride, as has been described in detail in an earlier publication[5]. The level of reversed monomeric units was controlled by the monomeric feed ratio in the copolymerization reaction, and was ascertained by 500 MHz ^1H n.m.r. Detailed assignment of regiosequences to the level of heptads was achieved[5] by using ^1H-decoupled 470 MHz ^{19}F n.m.r. in conjunction with two-dimensional *J*-correlated ^{19}F n.m.r. at 188 MHz.

For structural analysis by X-ray diffraction, the specimens were compression-moulded into flat films (*ca.* 200 μm) and then placed on specially designed resistive heating stages of a diffractometer or of a flat-plate vacuum camera. The indicated temperatures had been calibrated with melting-point standards to ±1°C. Nickel-filtered Cu Kα radiation was used. During diffractometry, the samples were scanned in the reflection geometry at 0.5–2° (2θ) min^{-1}.

RESULTS AND DISCUSSION

The room-temperature structure of PVF_2 as a function of regiodefect content may be studied by referring to *Figure 1*, which shows X-ray diffractograms in the reciprocal-space region of the major *inter*molecular (*hk*0) peaks. The sample having a regiodefect content of 5.1 mol% (typical of commercially available PVF_2) shows the expected α-phase peaks identified in this figure. For 11.4 mol%

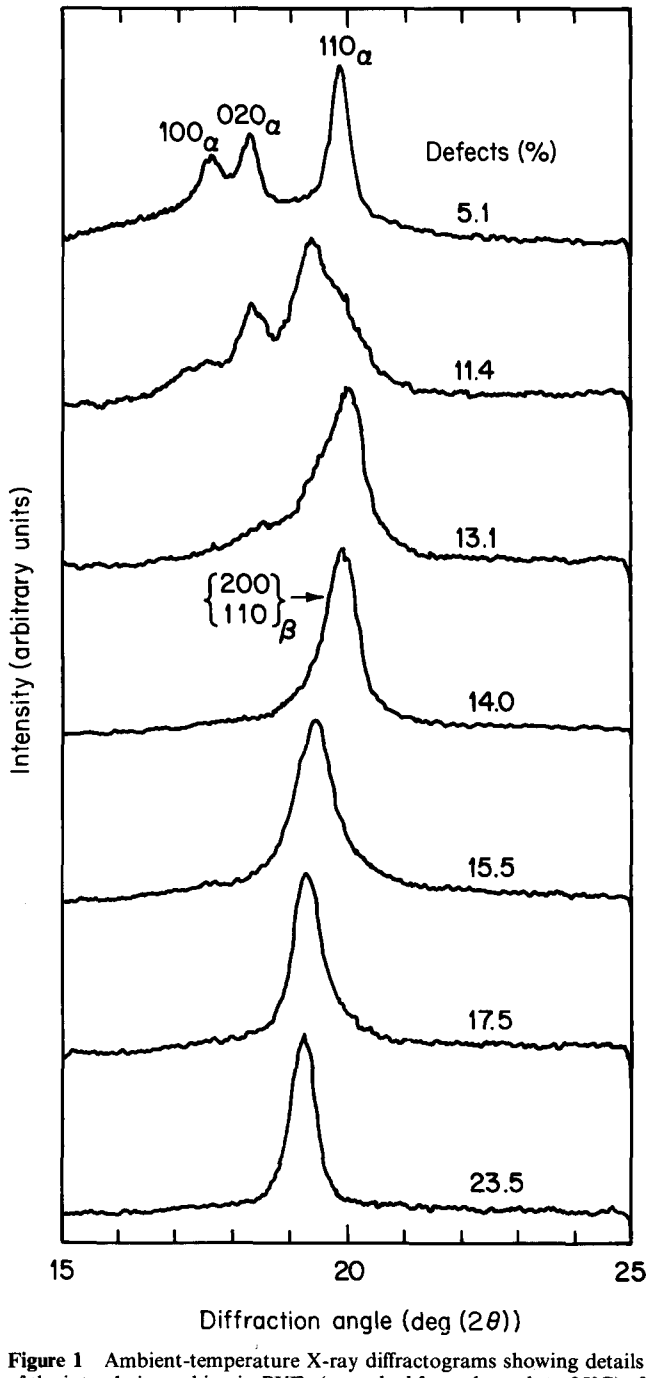

Figure 1 Ambient-temperature X-ray diffractograms showing details of the interchain packing in PVF_2 (quenched from the melt to 25°C) of varying defect content

defects a shoulder at *ca.* 20° (2θ), characteristic of the combined (200, 110) reflections of the β-phase, is seen. At 13.1% defects, β-PVF_2 becomes the dominant phase and the α-peaks are observed only as shoulders, while at 14.0% all vestiges of the α-phase have disappeared. At higher defect levels, the intermolecular packing appears to remain characteristic of β-PVF_2.

Figure 2 presents the same type of evidence from a wider range of 2θ, which allows probing of the molecular conformation (much of the detail from *Figure 1* is now lost). Peaks associated with the *trans*-conformation of β-PVF_2 (i.e. 001 and (201, 111)) become prominent at 13.1 and 14.0 mol% defects, while those related to the tg^+tg^- conformation of the α-phase disappear. However, it is important to note that the above reflections of the *trans*-

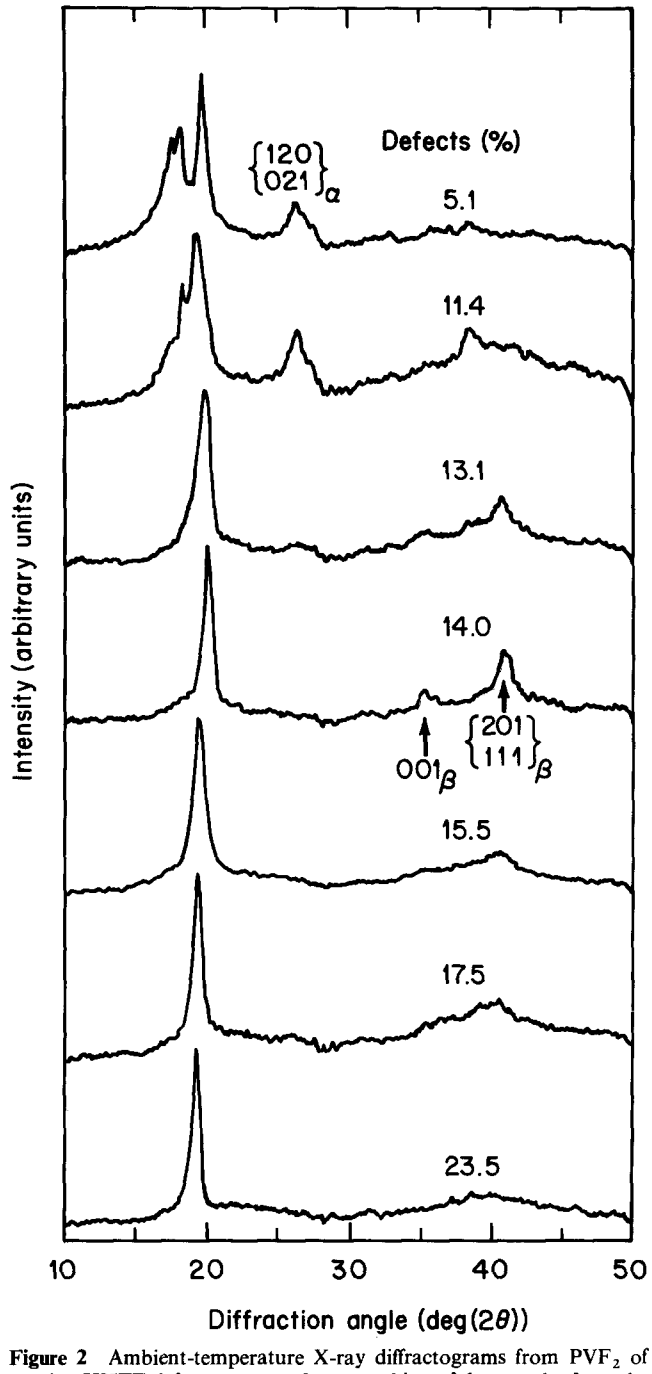

Figure 2 Ambient-temperature X-ray diffractograms from PVF_2 of varying HHTT defect content, after quenching of the samples from the melt to 25°C

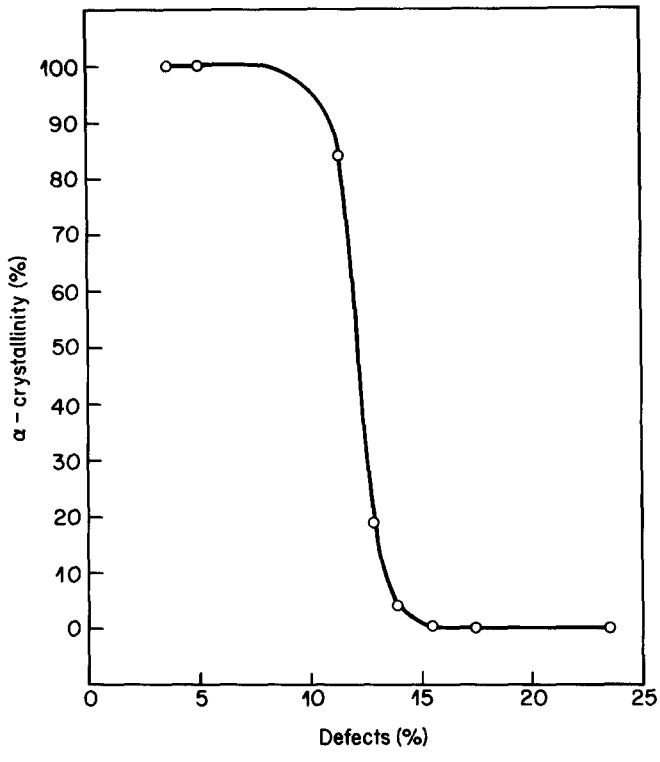

Figure 3 Relative extent of α-crystallinity as a function of HHTT defect content in PVF_2 specimens that had been quenched from the melt to 25°C

conformation become weaker and eventually indistinguishable as the defect content increases beyond *ca.* 15.5 mol%. This belies the apparent impression from *Figure 1* that the β-structure persists unchanged above the $\alpha \rightarrow \beta$ transition. In *Figure 2*, as well as in photographic diffraction patterns (which, for brevity, are not shown here), the meridional and off-meridional reflections from the *trans*-conformation are progressively replaced by a very broad peak centred at *ca.* 40° (2θ). This indicates the adoption of an increasingly disordered molecular conformation, as occurs in polytetrafluoroethylene (PTFE) above its disordering transition at 30°C[30], or in the paraelectric phase of PVF_2 copolymers[19]. Moreover, the intermolecular peak at *ca.* 19° (2θ) becomes significantly narrower with increasing defect content, approaching the sharpness characteristic of PTFE (this will be discussed further in relation to *Figure 5*).

An estimate of the relative proportion of the α-polymorph within the crystalline phase was obtained by separation of the intermolecular peaks from *Figure 1* that correspond to the two phases. Such an estimate of relative α-crystallinity as a function of HHTT content is given in *Figure 3* for specimens that had been quenched to room temperature (behaviour under different crystallization conditions is described later). Specimens with the usual number of defects (3.5–6.0 mol%) are fully in the α-phase, although under special conditions (e.g. at high pressures[31], epitaxy[32], or in ultra-thin (under 100 nm) films[33]) the β-polymorph may predominate. Since compositions between 5.1 and 11.4% regiodefects were not available, the exact point of departure from full α-crystallinity is not known. However, a sharp reversal in the α/β crystalline ratio is clearly seen as the defect content increases from 11.4 to 13.1 mol%. This first

experimental test of polymorphism *versus* HHTT content thus confirms quantitatively the long-standing prediction of Farmer *et al.*[4] based upon molecular energetics.

In *Figure 4*, we summarize the influence of defects on the *d*-spacing of the intermolecular lattice. Below *ca.* 6%, the defect population is too small to affect the lattice dimension, and the HHTT units are presumably accommodated as crystallographic point defects. At higher contents the incorporated reversed monomeric units cause a significant lattice expansion, which, however, is moderated above *ca.* 17%, indicating a saturation effect. As a comparison, data points are also included for PTFE and syndioregic PVF_2 (for the first, the 1 0 0 peak of the metrically hexagonal phase[30] at 25° is used, and for the second, the unresolved 2 0 0, 0 2 0 peak of its nearly tetragonal phase)[34]. Syndioregic PVF_2 is the alternating copolymer of ethylene and tetrafluoroethylene[34], and may be viewed as containing 50% reversed monomeric units or 100% HHTT groups. In this context, its *d*-spacing in *Figure 4* may be considered an upper limit for our regiodefective polymers. The corresponding spacing for PTFE is even higher since this polymer is equivalent to 100% HH units (without any of the smaller TT ($-CH_2-CH_2-$) groups). The influence of regiodefect content on crystal perfection can be estimated from the integral widths of the well-resolved *hk*0 reflections in *Figure 1* (after subtraction of instrumental broadening). To eliminate the effects of polymorphism, we show such estimates in *Figure 5* only for defect contents over 13.1 mol%. Because of the superposition of the 2 0 0 and 1 1 0 peaks and of the absence of multiple reflection orders, the effects of lattice distortions cannot be separated from those of crystallite size, as in the treatments of Bonart *et al.*[35] or Buchanan and Miller[36]. However, for these low-order peaks, the overall broadening reflects primarily crystallite size, i.e. in this case, the intermolecular coherence length over which correlations about the relative positions of the chain persist. This coherence length is seen in *Figure 5* to increase with defect content, which might at first appear

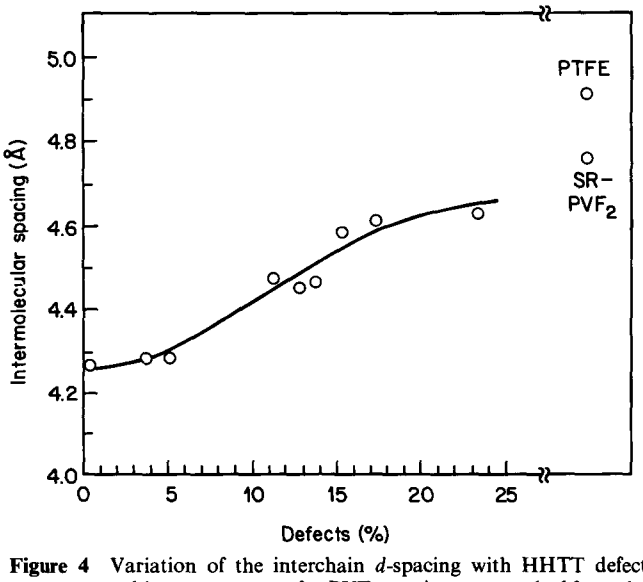

Figure 4 Variation of the interchain *d*-spacing with HHTT defect content at ambient temperature for PVF_2 specimens quenched from the melt to 25°C. The *d*-spacing shown originates from the (2 0 0, 1 1 0) reflection of β-PVF_2. For comparison, the corresponding spacings at 25°C are also shown for polytetrafluoroethylene (PTFE) d_{100} and syndioregic PVF_2 (SR-PVF_2) $d_{200,020}$

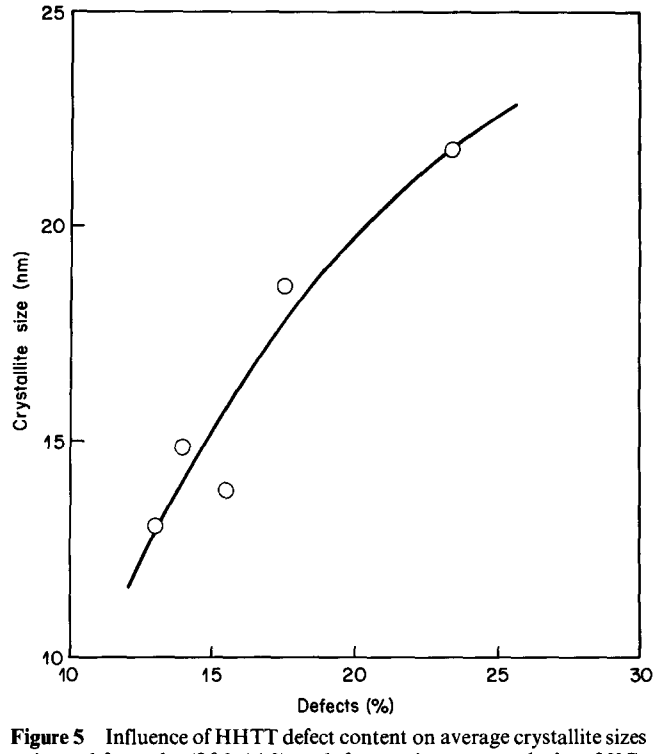

Figure 5 Influence of HHTT defect content on average crystallite sizes estimated from the (2 0 0, 1 1 0) peak for specimens quenched to 25°C

surprising. However, in a pseudo-hexagonal lattice of chains having distinctly anisometric cross-sectional profiles (as in β-PVF_2), any reduction in this anisometry will tend to improve the interchain packing. Introduction of additional regioirregularities accomplishes that and leads progressively to improved quasi-hexagonal packing. Such cases where *intra*molecular disorder is associated with high *inter*molecular order are well known among polymers (e.g. polytetrafluoroethylene[30], polytrifluoroethylene[37], the paraelectric phase of PVF_2 copolymers[19] and, more recently, the high-temperature phase of some polysilanes[38]).

The results described so far pertain to specimens that had all been crystallized by quickly cooling to ambient temperature. However, different crystallization treatments can be expected to have an effect on the polymorphism of PVF_2. The largest such effect was obtained for the 11.4% composition, as anticipated from its location on the steepest part of the curve in *Figure 3*. Samples quenched rapidly to very low or ambient temperatures (curves A and B in *Figure 6*) show a large preponderance of the α-phase. Slower crystallization at high temperatures increasingly favours the β-phase, yielding approximately equal populations of the two polymorphs (curve C). Growth at high temperatures for long periods of time (curve D) leads to a distinct dominance of the β-phase. The other compositions are much less sensitive to crystallization procedure with regard to polymorphism. PVF_2 samples having over 14.0 mol% HHTT defects show no changes in their diffraction patterns under a variety of crystallization programs similar to those described above for 11.4%. The 13.1% specimen, which contains only a small proportion of the α-phase when quenched in isopentane at -156°C or in air at 25°C (see also *Figures 1–3*), crystallizes fully in the β-phase at higher growth temperatures.

Having examined the room-temperature structure of PVF_2 as a function of regioregularity, we will now discuss

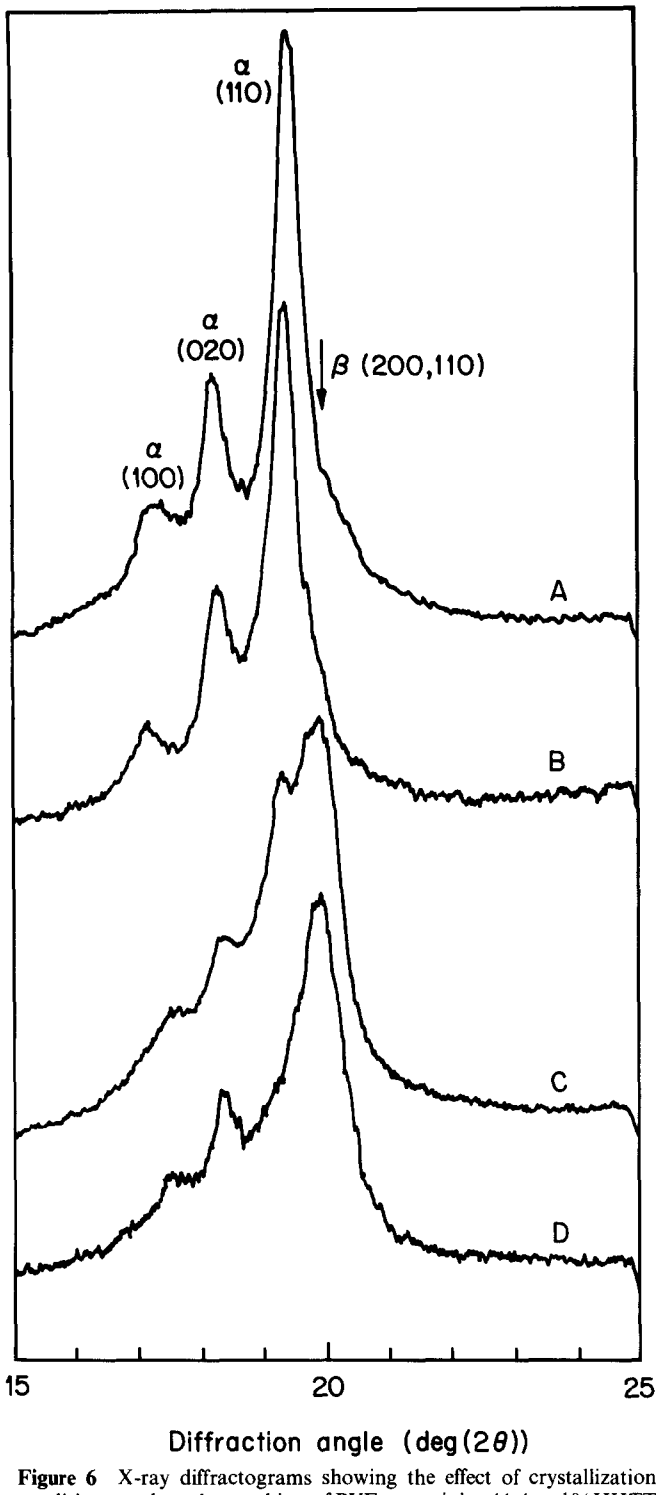

Figure 6 X-ray diffractograms showing the effect of crystallization conditions on the polymorphism of PVF_2 containing 11.4 mol% HHTT defects. A, Molten sample quenched in isopentane at −156°C, and, B, in air at 25°C. C, Sample crystallized from the melt by cooling at 10 K min^{-1} to ambient temperature, or, D, by isothermal growth at 130°C for 14 h

its variation with temperature during heating and cooling, paying particular attention to all evidence for Curie and other solid-state transitions. We will do so in greater detail for the 13.1% composition (whose transitional behaviour will be shown to be very similar to that found previously[19,26,27] for PVF_2 copolymers with tri- and tetrafluoroethylene), and will then describe the behaviour of other regiodefective samples more briefly and in relation to that of the 13.1% polymer. Unless otherwise described, all diffractograms shown from this point on originate from specimens that had been crystallized by quenching in air to 25°C. Such diffractograms are seen for the 12.1% HHTT polymer in *Figure 7*. The reciprocal-space region covered encompasses the strongest intermolecular-lattice peaks, which at ambient temperature consist primarily of the (2 0 0, 1 1 0) of the ferroelectric β-phase at *ca.* 20° (2θ), with a very small overlapping contribution from the antipolar α-phase. Heating of this specimen is clearly shown to cause a progressive decrease in the intensity of this ferroelectric-phase peak with a concomitant appearance and growth of a new peak at *ca.* 18° (2θ). In both reciprocal spacing and thermal behaviour during heating, this new peak is totally reminiscent of the *paraelectric* phase that we have previously examined in VF_2/F_3E and VF_2F_4E copolymers[19,26,27,39]. The high-temperature phase is seen to reach maximum proportions at 140°C (although the ferroelectric phase is not fully eliminated before melting); further heating causes the reduction and eventual disappearance of both peaks as a result of melting. Upon cooling, the high-temperature phase grows directly from the melt and persists, with only minimal presence of the ferroelectric phase, down to 80°C. With further cooling, the reverse transformation back to the original room-temperature structure is obtained. The X-ray features of the high-temperature phase during cooling, i.e. its preferred growth directly from the melt, its metastability to low temperatures and

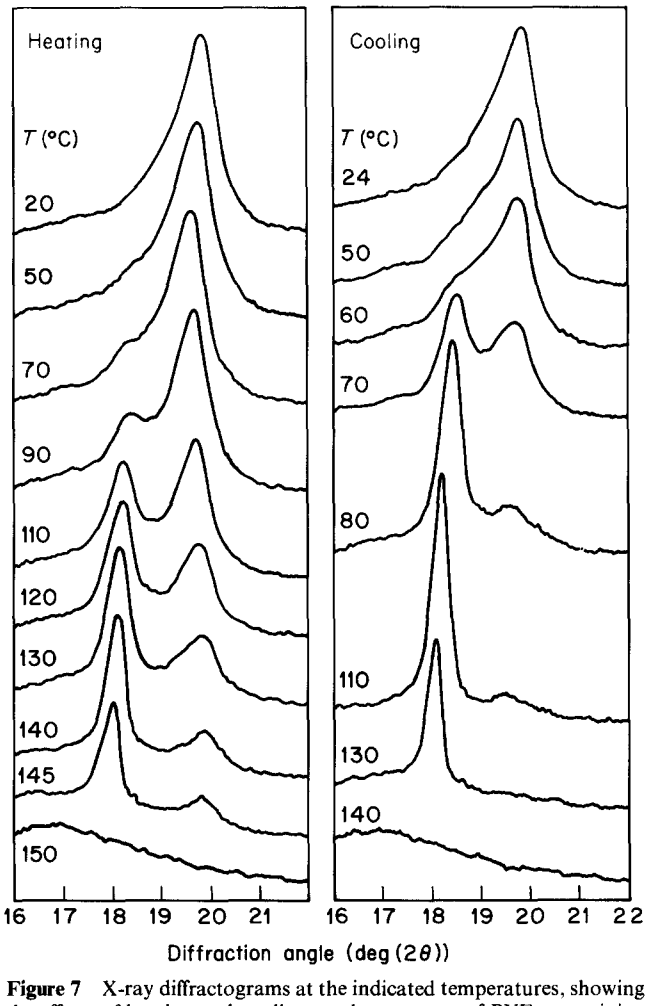

Figure 7 X-ray diffractograms at the indicated temperatures, showing the effects of heating and cooling on the structure of PVF_2 containing 13.1 mol% HHTT defects

the resulting hysteresis over a full thermal cycle, as well as the narrowness of its intermolecular peak, are all once again characteristic of the paraelectric phase found in the copolymers. The sharp peak profile is especially noteworthy when compared with that of the ferroelectric β-phase. The paraelectric phase in PVF_2 copolymers is known to result from introduction of $g^{\pm}$ bonds, leading to a statistical mixture of tg^+, tg^-, and tt sequences[8,9,19]. This irregular incorporation of $g^{\pm}$ bonds, as well as the rotational motions evident in the dielectric spectra[40-42], cause the molecules of the paraelectric phase to be packed in an expanded pseudo-hexagonal lattice; the molecular outline in c-axis projection is effectively cylindrical, leading to very efficient interchain packing and concomitantly narrow X-ray peaks, as seen also in *Figure 7*.

To ascertain that the high-temperature phase for this regiodefective PVF_2 is indeed equivalent to the paraelectric phase found in the VF_2/F_3E and VF_2/F_4E copolymers, we examined the full X-ray diffraction pattern by using a vacuum camera. The temperature variation of this pattern is seen at two different levels of exposure in *Figure 8*. At 25°C, the pattern is dominated by the strong inner reflection at $d=4.47$ Å studied in *Figure 7* and attributed to the (200,110) planes of the ferroelectric phase (with a small admixture of α-PVF_2 that is not resolved). At increasing radii, a weak (021,120) reflection of the α-phase is seen, followed consecutively by the (001) and (201,111) of the ferroelectric β-phase ($d=3.33$, 2.54 and 2.20 Å, respectively). Other α-phase reflections are also present, but too weak to be observed in *Figure 8a*. We will concentrate our attention on the outer β-phase reflections since they provide information about the (initially all-

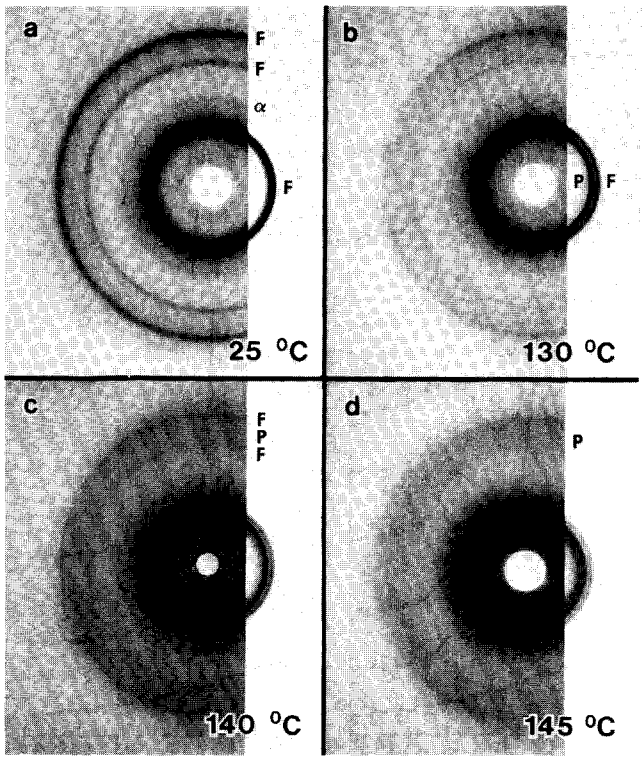

Figure 8 Vacuum-camera diffraction patterns of PVF_2 containing 13.1 mol% HHTT defects, recorded at four different temperatures during heating. F, ferroelectric (β) phase; P, paraelectric phase; α, α-phase

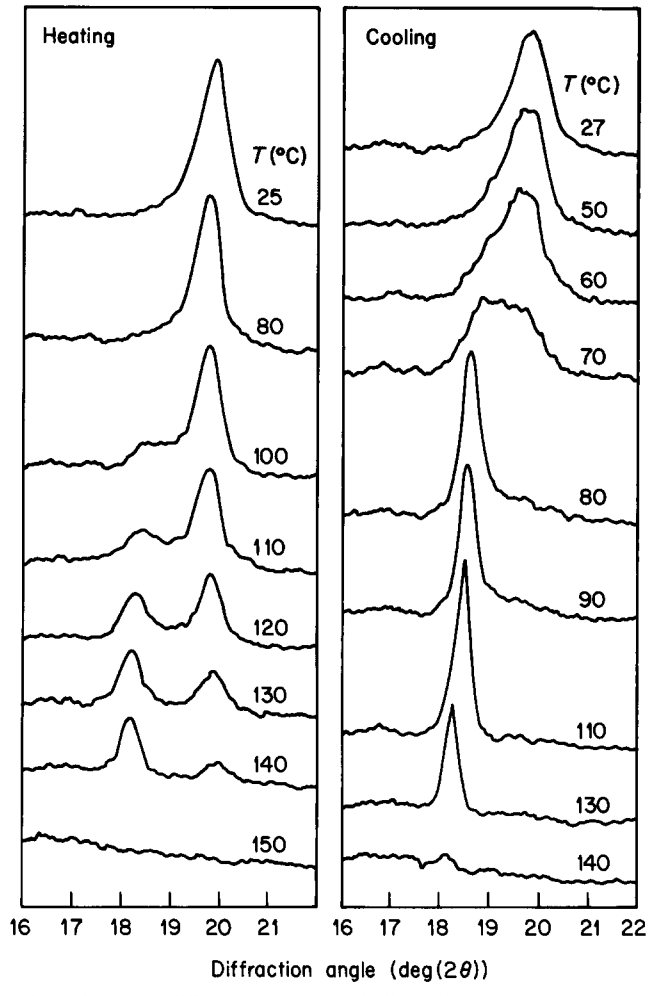

Figure 9 X-ray diffractograms at the indicated temperatures, showing the effects of heating and cooling on the structure of PVF_2 containing 14.0 mol% HHTT defects

trans) chain conformation. At 130°C (*Figure 8b*), the emergence of the intermolecular paraelectric-phase peak discussed above is seen to be accompanied by an increasing diffuseness in the region between the weakened (001) and (201,111) ferroelectric-phase reflections. The progressive replacement of these reflections by the diffuse peak (which is centred at *ca.* 2.30 Å) becomes more distinct as the temperature is increased further (*Figure 8c, d*). This is exactly the same behaviour as exhibited by the F_3E and F_4E copolymers of PVF_2. The broad reflection at 2.30 Å is characteristic of the molecular repeat of disordered chains consisting of irregular successions of tg^+, tg^- and tt groups. This shows not only that the high-temperature phase of PVF_2 with 13.1% regiodefects is indeed paraelectric, but also that it has a similar conformation, as found previously in the copolymers. We consider this a strong substantiation of the validity of our previous descriptions of the Curie transition in VF_2/F_3E and VF_2/F_4E copolymers as representative of the properties of PVF_2 *itself*.

With this knowledge from the 13.1% HHTT material, we now move on to more regiodefective PVF_2 compositions. In *Figure 9* are shown diffractograms for the 14.0% polymer recorded at different temperatures during the heating and cooling cycle. The behaviour is as described for *Figure 7*, with the exception of a more limited conversion to the paraelectric phase upon heating. The cooling curves are remarkably similar to

those of the 13.1% sample, and show both a strong initial crystallization in the paraelectric phase and its conversion to the ferroelectric phase at *ca.* 70°C.

The 15.5 mol% HHTT sample (*Figure 10*) also exhibits the ferroelectric–paraelectric transformation during heating, with the two phases coexisting to different extents over a wide range of temperature. The narrowness of the paraelectric peak upon cooling is remarkable. Also noteworthy is the fact that the reverse transition is not fully completed when the sample is cooled to ambient temperature. The significant presence of the paraelectric phase at 29°C is attributed to the annealing treatment inherent in the cooling programme of *Figure 10*; quenching to 26°C (as seen in the same figure) yields exclusively the ferroelectric phase.

Beyond 15.5 mol% regiodefects, the structural changes during a heating and cooling cycle are small and indicate no signs of a Curie transition. For the sake of brevity, *Figure 11* illustrates X-ray diffractograms for the polymer containing 17.5 mol% HHTT units (the behaviour of the 23.5 mol% material is essentially the same). The structure at room temperature has already been described in relation to *Figure 2*, and its departure from that of the ferroelectric phase as a result of significant disorder has been noted. We therefore consider the structure of polymers with over 17.5 mol% regiodefects to be similar to the paraelectric at all temperatures studied; further

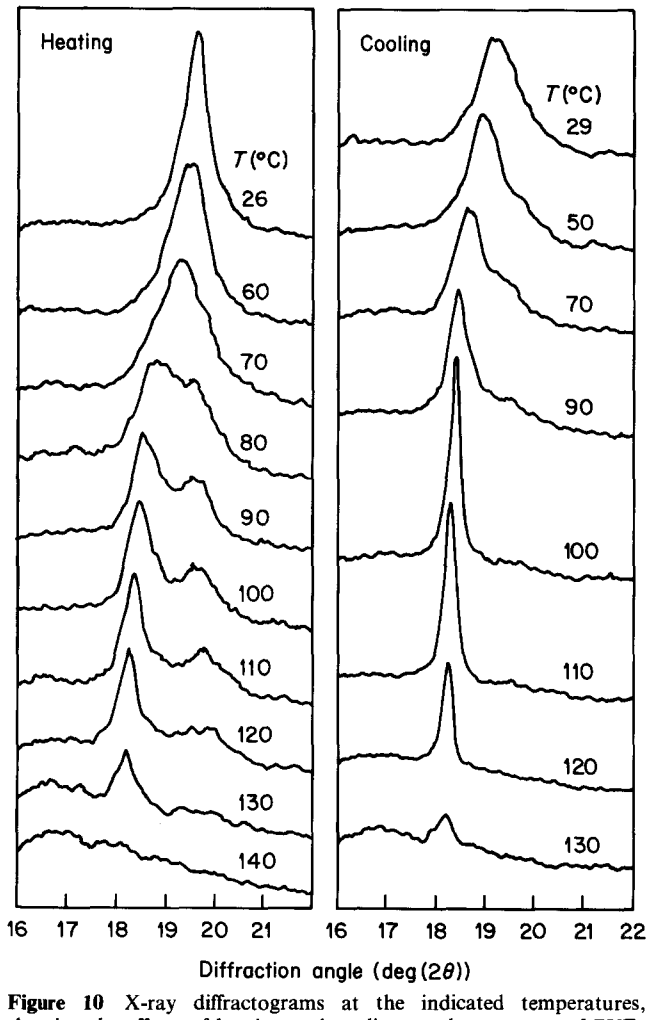

Figure 10 X-ray diffractograms at the indicated temperatures, showing the effects of heating and cooling on the structure of PVF_2 containing 15.5 mol% HHTT defects

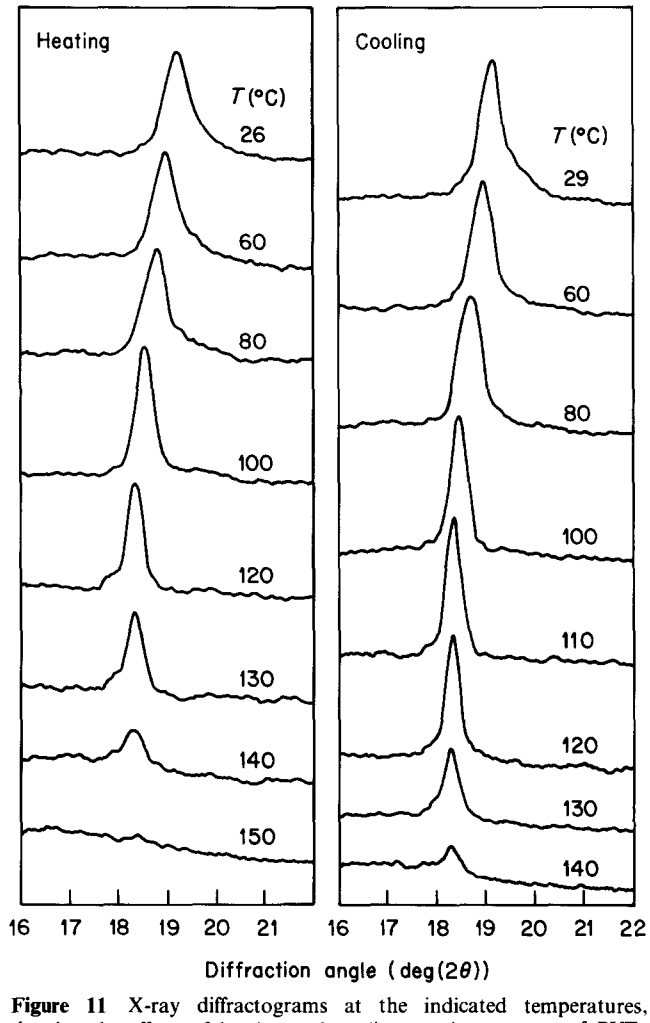

Figure 11 X-ray diffractograms at the indicated temperatures, showing the effects of heating and cooling on the structure of PVF_2 containing 17.5 mol% HHTT defects

confirmation of this in terms of the temperature variation of interplanar spacings is given in *Figure 12*.

Figure 12 summarizes the measured (200, 110) *d*-spacings of the four compositions described so far (i.e. 13.1–17.5 mol% regiodefects). The 13.1 and 14.0% polymers (*Figure 12a, b*) show similar thermal behaviour and interplanar spacings. While their paraelectric phases undergo significant expansion during heating, their ferroelectric counterparts show little change in *d*-spacing and, if anything, a very slight contraction at high temperatures. This surprising phenomenon is substantiated more clearly and pronouncedly for the 15.5 mol% specimens (*Figure 12c*). Here, the initial room-temperature structure obtained by quenching exhibits a large lattice spacing as a result of incorporation of the defects within the crystalline regions. After expansion of this defective structure to 70°C and initiation of the Curie transition, the remaining ferroelectric phase is packed in an increasingly compact lattice, presumably because of preferential rejection of defects into the paraelectric phase (whose lattice expands greatly). Upon cooling, this behaviour is reversible to a large extent, although the ferroelectric phase at room temperature is now more compact than originally; this is attributable to the slow cooling treatment and the resulting survival of the paraelectric phase, in which most of the defects are expected to reside. For the 17.5 mol% HHTT PVF_2, the interplanar spacings of the sole observed phase (*Figure*

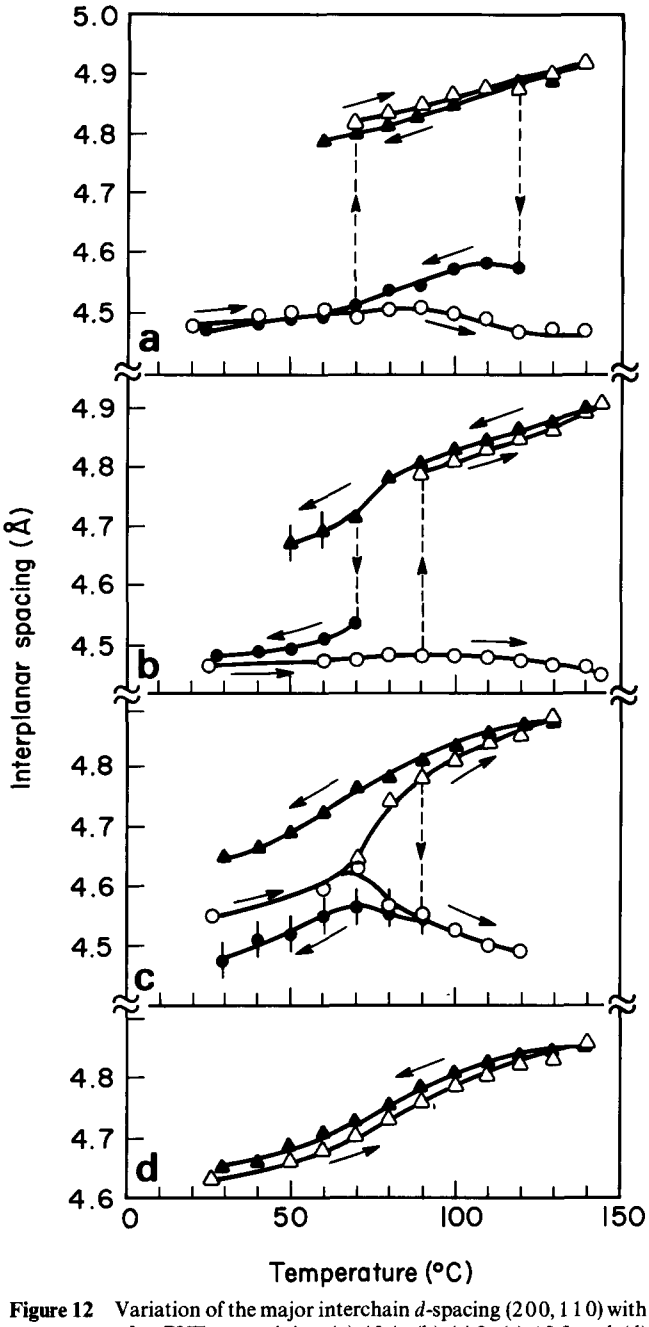

Figure 12 Variation of the major interchain *d*-spacing (2 0 0, 1 1 0) with temperature for PVF_2 containing (a) 13.1, (b) 14.0, (c) 15.5 and (d) 17.5 mol% HHTT defects: ○, ●, ferroelectric phase; △, ▲, paraelectric phase; ○, △, heating; ●, ▲, cooling

12d) are characteristic of the paraelectric polymorph. In fact, the curves of *Figure 12d* are virtually superimposable on the paraelectric curves of *Figures 12b, c*, suggesting that, above ambient temperature, PVF_2 having over 17.5 mol% defects exists only in a structure similar to the paraelectric. It is possible that a ferroelectric phase might exist at lower temperatures, but we have not observed it at temperatures as low as −10°C (which is our experimental limit for diffractometry).

Having examined the structural changes induced by heating and cooling in PVF_2 of defect content above 13.1 mol%, we now investigate the behaviour of less regiodefective samples. X-ray difrractograms for nominally isoregic PVF_2 (0.2 mol% HHTT) are seen in *Figure 13*. As expected, this polymer adopts the α-phase structure when quenched to ambient temperature from the melt,although, surprisingly, a small amount of the β-polymorph is also obtained. Reasons for presence of the β-phase, whether associated with the ultralow defect content or with the low molecular weight and the effect of chain ends (crystals being in all probability chain-extended), are not known at present. The room-temperature structure persists with no conversion to a paraelectric phase as the material is heated to the melting point. When the sample is subsequently crystallized from the melt, the α-phase is grown directly; a significant minority of β-type crystals appears as the temperature is lowered below *ca.* 100°C. Specimens predominately in the β-phase could not be obtained, since the very low molecular weight made drawing impossible.

The final composition used contained 11.4% defects, which is of particular interest because (as was discussed in relation to *Figure 6*) it normally adopts the α-structure, but can also be made to crystallize predominately in the β-phase. We illustrate its crystallographic changes during heating and cooling in *Figure 14* by using a specimen that is mostly in the α-phase, but which also contains a large fraction of β-crystals, so as to probe the behaviour of both polymorphs. The initial diffractogram at room temperature shows the usual $(1\,0\,0)_\alpha$, $(0\,2\,0)_\alpha$, $(1\,1\,0)_\alpha$ and $(2\,0\,0, 1\,1\,0)_\beta$ peaks in increasing order of 2θ. As the specimen is heated to 80°C and then 90°C, a number of remarkable changes is seen. The $(1\,0\,0)_\alpha$ and $(1\,1\,0)_\alpha$ peaks are diminished greatly, while the corresponding $(0\,2\,0)_\alpha$ peak shows a slight increase. This increase is attributed to

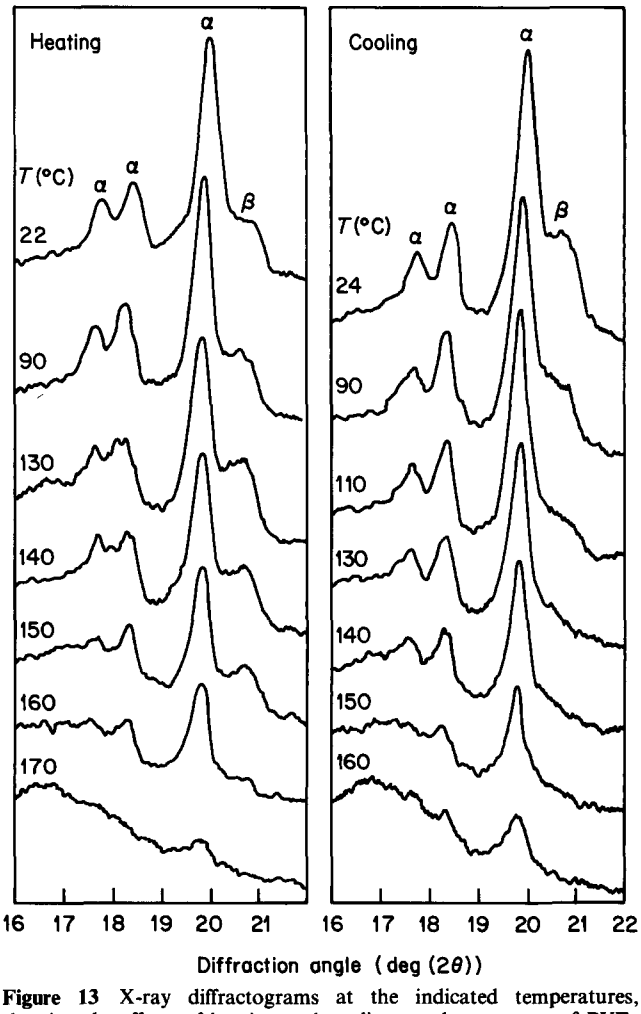

Figure 13 X-ray diffractograms at the indicated temperatures, showing the effects of heating and cooling on the structure of PVF_2 containing 0.2 mol% HHTT defects

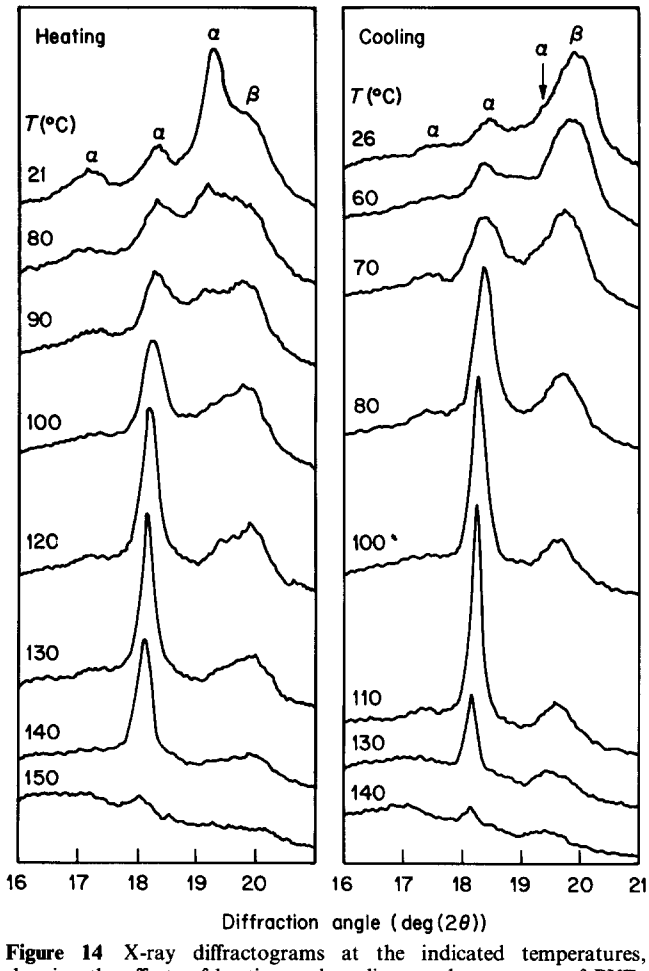

Figure 14 X-ray diffractograms at the indicated temperatures, showing the effects of heating and cooling on the structure of PVF_2 containing 11.4 mol% HHTT defects

the emergence of the paraelectric peak at the same spacing, as is evident when the sample is heated to successively higher temperatures. It is important to note that the β-peak remains close to its original intensity as the α-peaks are drastically reduced. To a large extent, therefore, the paraelectric phase is being generated at the expense of the antipolar α-phase and not of the ferroelectric β-phase. This surprising finding implies that the observed structural changes result not from a true Curie transition, but rather from a more general solid-state phase transformation. Apparently, the disordered conformation and accompanying efficient packing of the paraelectric phase are energetically more favourable at high temperatures than either their α- or β-counterparts for 11.4% HHTT PVF_2. As this polymer is cooled, crystallization occurs as expected, i.e. primarily into the paraelectric lattice and with only a small contribution to the β-phase. Further lowering of temperature leads to a transformation to the β-polymorph. The reason that only a small minority of α-crystals is seen after return to ambient temperature (contrary to the original structure) is that slow crystallization favours the β-polymorph (as discussed in relation to *Figure 6*).

CONCLUSIONS

We have shown in this series of regiodefective PVF_2 polymers that their room-temperature structure exhibits a smooth progression from α, to mixtures of α and β (between *ca.* 11.4 and 13.1 mol% HHTT defects), to β (up to *ca.* 15.5% defects) and finally to a paraelectric-like phase consisting of conformationally disordered chains that are packed quasi-hexagonally with high intermolecular order. The relative β/α ratio at intermediate defect levels (11.4–13.1%) increases with HHTT content and with temperature of crystallization. The lattice spacing and intermolecular coherence length also increase as more defects are incorporated into the chains. When heated, copolymers with 13.1–15.5 mol% HHTT units undergo Curie transitions from the ferroelectric phase to a disordered paraelectric one. During this process, HHTT units may be preferentially rejected to the paraelectric phase, leading to contraction of the ferroelectric lattice at high temperatures. Upon subsequent cooling, the paraelectric phase crystallizes first and then undergoes a reverse transition back to the ferroelectric, in the same manner as shown previously for PVF_2 copolymers with F_3E and F_4E. This demonstrates that our conclusions from the two series of copolymers are indeed valid and reflect the inherent behaviour of PVF_2 itself and not of the comonomers. For the isoregic polymer and for the aregic ones with HHTT content over 17.5 mol%, no phase transformations are seen. The 11.4 mol% polymer shows a transformation to the paraelectric phase when heated, but interestingly, that occurs mainly at the expense of the antipolar α-phase (rather than the ferroelectric β), and is therefore not a Curie transition.

REFERENCES

1 Cais, R. E. and Sloane, N. J. A. *Polymer* 1983, **24**, 179
2 Görlitz, M., Minke, R., Trautvetter, W. and Weisgerber, G. *Angew. Makromol. Chem.* 1973, **29/30**, 137
3 Wilson, C. W. III *J. Polym. Sci. A* 1963, **1**, 1305
4 Farmer, B. L., Hopfinger, A. J. and Lando, J. B. *J. Appl. Phys.* 1972, **43**, 4293
5 Cais, R. E. and Kometani, J. M. *Macromolecules* 1985, **18**, 1354
6 Lando, J. B. and Doll, W. W. *J. Macromol. Sci.–Phys.* 1968, **B2**, 205
7 Lovinger, A. J. *Science* 1983, **220**, 1115
8 Lovinger, A. J. *Jpn. J. Appl. Phys.* 1985, **24**(2), 18
9 Tashiro, K. and Kobayashi, M. *Jpn. J. Appl. Phys.* 1985, **24**(2), 873
10 Furukawa, T., Date, M. and Fukada, E. *J. Appl. Phys.* 1980, **51**, 1135
11 Tashiro, K., Takano, K., Kobayashi, M., Chatani, Y. and Tadokoro, H. *Polymer* 1983, **24**, 199
12 Tashiro, K., Takano, K., Kobayashi, M., Chatani, Y. and Tadokoro, H. *Polym. Bull.* 1983, **10**, 464
13 Yagi, T., Tatemoto, M. and Sako, J. *Polym. J.* 1980, **12**, 209
14 Furukawa, T., Johnson, G. E., Bair, H. E., Tajitsu, Y., Chiba, A. and Fukada, E. *Ferroelectrics* 1981, **32**, 61
15 Yamada, T., Ueda, T. and Kitayama, T. *J. Appl. Phys.* 1981, **52**, 948
16 Tashiro, K., Takano, K., Kobayashi, M., Chatani, Y. and Tadokoro, H. *Polymer* 1981, **22**, 1312
17 Lovinger, A. J., Davis, G. T., Furukawa, T. and Broadhurst, M. G. *Macromolecules* 1982, **15**, 323
18 Davis, G. T., Furukawa, T., Lovinger, A. J. and Broadhurst, M. G. *Macromolecules* 1982, **15**, 329
19 Lovinger, A. J., Furukawa, T., Davis, G. T. and Broadhurst, M. G. *Polymer* 1983, **24**, 1225, 1233
20 Tashiro, K. and Kobayashi, M. *Polymer* 1986, **27**, 667
21 Matsushige, K., Horiuchi, T., Taki, S. and Takemura, T. *Jpn. J. Appl. Phys.* 1985, **24**, L203
22 Koizumi, N., Murata, Y. and Haikawa, N. *Jpn. J. Appl. Phys.* 1985, **24**(2), 862
23 Lovinger, A. J. *Macromolecules* 1985, **18**, 910
24 Odajima, A., Takase, Y., Ishibashi, T. and Yuasa, K. *Jpn. J. Appl. Phys.* 1985, **24**(2), 881
25 Lovinger, A. J. *Macromolecules* 1983, **16**, 1529

26 Lovinger, A. J., Johnson, G. E., Bair, H. E. and Anderson, E. W. *J. Appl. Phys.* 1984, **56**, 2412
27 Lovinger, A. J., Davis, D. D., Cais, R. E. and Kometani, J. M. *Macromolecules* 1986, **19**, 1491
28 Murata, Y. and Koizumi, N. *Polym. J.* 1985, **17**, 1071
29 Cais, R. E. and Kometani, J. M. *Org. Coat. Appl. Polym. Sci. Proc. Am. Chem. Soc.* 1983, **48**, 216
30 Clark, E. S. and Muus, L. T. *Z. Krist.* 1962, **117**, 119; see also Weeks, J. J., Eby, R. K. and Clark, E. S. *Polymer* 1981, **22**, 1496
31 Scheinbeim, J., Nakafuku, C., Newman, B. A. and Pae, K. D. *J. Appl. Phys.* 1979, **50**, 4399
32 Lovinger, A. J. *Polymer* 1981, **22**, 412
33 Hsu, C. C. and Geil, P. H. *Polymer* 1986, **27** (*Commun.*), 105
34 Wilson, F. C. and Starkweather, H. W. Jr *J. Polym. Sci., Polym. Phys. Edn.* 1973, **11**, 919
35 Bonart, R., Hosemann, R. and McCullough, R. L. *Polymer* 1963, **4**, 199
36 Buchanan, D. R. and Miller, R. L. *J. Appl. Phys.* 1966, **37**, 4003
37 Lovinger, A. J. and Cais, R. E. *Macromolecules* 1984, **17**, 1939
38 Lovinger, A. J., Schilling, F. C., Bovey, F. A. and Zeigler, J. M. *Macromolecules* 1986, **19**, 2657
39 Lovinger, A. J., Cais, R. E., Bair, H. E., Johnson, G. E., Davis, D. D., Kometani, J. M. and Anderson, E. W. *Bull. Am. Phys. Soc.* 1986, **31**, 611
40 Furukawa, T. and Johnson, G. E. *J. Appl. Phys.* 1981, **52**, 940
42 Ohuchi, M., Chiba, A., Date, M. and Furukawa, T. *Jpn. J. Appl. Phys.* 1983, **22**, 1267
42 Furukawa, T., Ohuchi, M., Chiba, A. and Date, M. *Macromolecules* 1984, **17**, 1384